

## Nonlinear response of Bloch electrons in finite dimensions

V. Turkowski and J. K. Freericks<sup>y</sup>

Department of Physics, Georgetown University, Washington, D.C. 20057

(Dated: April 14, 2024)

The exact nonlinear response of noninteracting (Bloch) electrons is examined within a nonequilibrium formalism on the finite-dimensional hypercubic lattice. We examine the effects of a spatially uniform, but time-varying electric field (ignoring magnetic-field effects). The electronic Green's functions, Wigner density of states, and time-varying current are all determined and analyzed. We study both constant and pulsed electric fields, focusing on the transient response region. These noninteracting Green's functions are an important input into nonequilibrium dynamical mean-field theory for the nonlinear response of strongly correlated electrons.

PACS numbers: 71.10.-w, 72.20.Ht, 71.45.Gm

## I. INTRODUCTION

The linear-response theory of Kubo<sup>1</sup> and Greenwood<sup>2</sup> is an attractive approach to understand how electrons (in the solid state) interact with external electromagnetic fields. It can be used (in principle) to calculate general linear-response functions in systems that have arbitrarily strong electron correlations. Surprisingly, the linear-response regime for many bulk materials (especially for parabolic band semiconductors<sup>3,4,5,6,7</sup>) and devices, holds for a wide range of electric field strengths.

But there are a multitude of interesting nonlinear effects in electric fields. Most electronic devices have a nonlinear current-voltage relation (transistors, Josephson junctions, etc.) and there is wide interest in nonlinear effects in bulk materials as well (since it is the nonlinearity that often determines the ultimate performance).

Devices are also becoming smaller and smaller. Semiconductor processing line features are well below 100 nm, and there is significant research effort on nanoscale devices. In the latter case, a potential difference of one volt produces an electric field on the order of  $10^7$  V/cm for nanometer scaled devices. These fields are large enough for nonlinear effects to be important, if not critical, to determine the proper behavior in an external field. There also has been significant research performed on high energy density pulsed laser experiments, where fields as high as  $10^{10}$  V/cm can easily be attained over a short time scale. In that case, one drives the material out of equilibrium by the pulse, and studies how it relaxes back to an equilibrium distribution (as a means to determine relaxation times, etc.).

There are few theoretical approaches to nonlinear effects in solid-state systems. The formalism was developed independently by Kadano and Baym<sup>8</sup> and Keldysh<sup>9,10</sup> in the early 1960s (Baym<sup>11</sup> and Keldysh<sup>12</sup> have each written short historical accounts of their discoveries). These approaches include the effects of external fields to all orders and typically use perturbation theory to determine the effects of many-body interactions<sup>13</sup>. In the 1980s, Wilkins and collaborators<sup>3,4,5,6,7,14,15,16</sup> spent much effort in developing these ideas further, and in examining nonlinear responses in finite dimensions. Here we extend

that work to finite-dimensional lattices, where we find many of the results for the electronic Green's functions can be determined analytically. Our formalism allows for an analysis of steady-state effects (like the Wannier-Stark ladders<sup>17</sup>) and of transient effects (like the response to a pulsed field). These noninteracting Green's functions are a necessary input to a complete nonlinear response dynamical mean-field theory for strongly correlated electrons. We will present results for that work in a separate publication.

The organization of this contribution is as follows: in Section II, we present the formalism for the nonlinear response, in Section III, we present our numerical results, and in Section IV, we present our conclusions.

## II. GREEN'S FUNCTIONS FOR BLOCH ELECTRONS IN AN EXTERNAL ELECTRIC FIELD

The Hamiltonian for tight-binding electrons hopping on a hypercubic lattice (in the absence of any external fields) is

$$H = \sum_{ij} t_{ij} c_i^\dagger c_j + \sum_i \epsilon_i c_i^\dagger c_i \quad (1)$$

where  $t_{ij}$  is the Hermitian hopping matrix (chosen to be<sup>18</sup>  $t_{ij} = t = 2\phi/d$  for nearest neighbors as  $d \rightarrow 1$ ), and

$\epsilon_i$  is the chemical potential. We shall consider the case when this system is coupled to an external electromagnetic field. An electromagnetic field is described by a scalar potential  $\phi(\mathbf{r};t)$  and a vector potential  $\mathbf{A}(\mathbf{r};t)$  via

$$\mathbf{E}(\mathbf{r};t) = -\nabla \phi(\mathbf{r};t) - \frac{1}{c} \frac{\partial \mathbf{A}(\mathbf{r};t)}{\partial t} \quad (2)$$

for the electric field, with  $c$  the speed of light. We will use the Landau gauge where  $\nabla \cdot \mathbf{A} = 0$  to perform our calculations, so the electric field is described solely by the vector potential. This provides a significant simplification of the formalism for spatially uniform (but possibly time-varying) electric fields.

Unlike many time-dependent Hamiltonians, the effect of the vector potential is not easily described by adding a time-dependent piece to the Hamiltonian in addition to the time-independent piece in Eq. (1). Instead, one uses the so-called Peierls' substitution<sup>15</sup> for the hopping matrix:

$$t_{ij} \rightarrow t_{ij} \exp \left[ \frac{ie}{\hbar c} \int_{R_i}^{R_j} A(r;t) dr \right]; \quad (3)$$

where  $R_i$  is the spatial lattice vector associated with lattice site  $i$  (and similarly for site  $j$ ) and  $e$  is the electric charge. Note that the Peierls' substitution is a simplified semiclassical treatment of the electromagnetic field (our vector potential is a classical, not quantum field) and we are ignoring dipole (and multipole) transitions between bands because we consider just a single-band model. In this case, the Hamiltonian of the noninteracting electrons coupled to an electromagnetic field becomes

$$H(t) = \sum_{ij} t_{ij} \exp \left[ \frac{ie}{\hbar c} \int_{R_i}^{R_j} A(r;t) dr \right] c_i^\dagger c_j \quad (4)$$

The corresponding electric field becomes

$$E(r;t) = -\frac{1}{c} \frac{\partial A(r;t)}{\partial t}; \quad (5)$$

We will choose the vector potential in such a way that either the field is zero before  $t = 0$  and is then turned on, or the field becomes asymptotically small as  $t \rightarrow \infty$  and it is adiabatically switched on; in this way, the early time Hamiltonian is always given by Eq. (1), and that will be used to establish the initial thermal equilibrium. The magnetic field has a complicated structure in infinite dimensions, because it involves the curl of the vector potential, which would need to be defined correctly for the infinite-dimensional limit. Because we are interested in electric fields with weak spatial dependence, we shall assume the associated magnetic field is small enough that we can neglect it, even though we will allow the electric field to vary in time. This is an approximation, because our electromagnetic fields no longer satisfy Maxwell's equations, unless the field is uniform in space and constant in time. This condition can be relaxed, perhaps by using a gradient expansion for the weak spatial dependence of the fields<sup>15</sup>, but such an approach is cumbersome in infinite dimensions. From now on, we neglect the spatial dependence of the vector potential (i.e., we are considering only spatially uniform but time-varying electric fields).

It is convenient to introduce a momentum-space representation for the Hamiltonian, which becomes

$$H(t) = \sum_k \left[ \epsilon(k) \frac{eA(t)}{\hbar c} \right] c_k^\dagger c_k; \quad (6)$$

with  $c_k = \frac{1}{\sqrt{N}} \sum_j c_j \exp[iR_j \cdot k]$  and  $c_k^\dagger = \frac{1}{\sqrt{N}} \sum_j c_j^\dagger \exp[-iR_j \cdot k]$ . Note that the Hamiltonian in Eq. (6) is a special time-dependent Hamiltonian, because it commutes with itself for all times  $[H(t); H(t^0)] = 0$ , which greatly simplifies the analysis of the time-dependent Green's functions developed below.

The expression for the time-ordered single-particle Green's function is defined to be

$$g^T(k;t;t^0) = \frac{i}{\hbar} T \langle c_k(t) c_k^\dagger(t^0) \rangle; \quad (7)$$

because of the special time dependence of the Hamiltonian, this Green's function can be determined analytically. In Eq. (7), the operators are expressed in a Heisenberg picture, where the time dependence is  $O(t) = \exp[iH(t)] O \exp[-iH(t)]$  with  $H(t)$  determined from Eq. (4), the time ordering symbol  $T$  orders earlier times to the right (with a change of sign when two Fermionic operators are interchanged), and the angle brackets indicate a thermal averaging  $\langle \dots \rangle = \text{Tr}[\exp(-\beta H) \dots] / \text{Tr}[\exp(-\beta H)]$ , with  $\beta = 1/T$  the inverse temperature and the Hamiltonian being the field-free (early-time) Hamiltonian from Eq. (1). We directly solve for the Green's function by finding the time dependence of the momentum-dependent creation and annihilation operators, and then directly solve for the Green's function by taking the relevant expectation values and traces<sup>15,19,20</sup>. The starting point is to calculate the time dependence of the operators:

$$\frac{d}{dt} c_k^\dagger(t) = \frac{i}{\hbar} \left[ c_k^\dagger(t), H(t) \right] = c_k^\dagger(t) \quad (8)$$

$$\frac{d}{dt} c_k(t) = \frac{i}{\hbar} \left[ c_k(t), H(t) \right] = -c_k(t) \quad (9)$$

which can be integrated to give

$$c_k^\dagger(t) = \exp \left[ \frac{i}{\hbar} \int_{t^0}^t \epsilon(k) \frac{eA(t')}{\hbar c} dt' \right] c_k^\dagger(t^0) \quad (10)$$

$$c_k(t) = \exp \left[ -\frac{i}{\hbar} \int_{t^0}^t \epsilon(k) \frac{eA(t')}{\hbar c} dt' \right] c_k(t^0) \quad (11)$$

It is now easy to find the expression for the time-ordered Green's function by inserting the time dependence from Eqs. (10) and (11) into the definition of the Green's function in Eq. (7) to yield

$$g^T(k;t;t^0) = \frac{i}{\hbar} \langle c_k(t) c_k^\dagger(t^0) \rangle = \frac{i}{\hbar} \langle \exp \left[ \frac{i}{\hbar} \int_{t^0}^t \epsilon(k) \frac{eA(t')}{\hbar c} dt' \right] c_k(t^0) c_k^\dagger(t^0) \exp \left[ -\frac{i}{\hbar} \int_{t^0}^t \epsilon(k) \frac{eA(t')}{\hbar c} dt' \right] \rangle = \frac{i}{\hbar} \langle f(k) \rangle = f(k); \quad (12)$$

since the averages satisfy  $\langle c_k^\dagger c_k \rangle = f(k)$  and  $\langle c_k c_k^\dagger \rangle = [1 - f(k)]$  with  $f(x) = [1 + \exp(\beta \epsilon(x))]^{-1}$  being the Fermi-Dirac distribution, and  $\epsilon(k)$  the band structure.

In finite-dimensional calculations, it is often important to also determine local properties, like the local Green's function  $g_{loc} = \langle g(k) \rangle$ , or the local density of states (DOS). The Green's function in Eq. (12) depends on both  $\mathbf{k}$  and  $\mathbf{k} \cdot \mathbf{e}_A = \tilde{c}$ . Hence, the summation over momentum cannot be performed simply by introducing an integral over the noninteracting DOS. Instead, the method of Mueller-Hartmann must be used<sup>21,22,23</sup>, to perform the integrations over the Brillouin zone and to extract the leading contributions as  $d \rightarrow 1$ . The algebra is straightforward, but lengthy. The final result is

$$g_{loc}^T(t; t^0) = \frac{i}{\tilde{c}} \int_{t^0}^t dt \left[ (t - t^0) f(\tilde{c}) \right. \\ \left. + \exp\left[-\frac{1}{\tilde{c}} \int_{t^0}^t dt \cos \frac{eaA(t)}{\tilde{c}}\right] \right. \\ \left. + \exp\left[\frac{t^2}{4\tilde{c}^2} - \frac{1}{\tilde{c}} \int_{t^0}^t dt \cos \frac{eaA(t)}{\tilde{c}}\right] \right. \\ \left. + \frac{1}{\tilde{c}} \int_{t^0}^t dt \int_{t^0}^t dt^0 \cos \frac{eaA(t) - A(t^0)}{\tilde{c}} \right] g^0 \\ e^{i(t-t^0)\tilde{c}}; \quad (13)$$

where  $\tilde{c}$  denotes the component of the vector potential and  $f(\tilde{c}) = \exp[-\tilde{c}^2 t^2] = \tilde{c}^{-d}$  is the noninteracting DOS (and  $a$  is the lattice spacing). Note that in the limit  $A \rightarrow 0$ , this reduces to the well-known noninteracting Green's function on a hypercubic lattice.

While the results of Eq. (13) are completely general, they are quite cumbersome for calculations, and it is useful to consider some simpler limits. The easiest case to evaluate, which is what we consider for the remainder of this paper, is to examine the case where the vector potential lies along the  $(1;1;1;...)$  diagonal  $A(t) = A(t)(1;1;1;...)$ . This choice simplifies the calculations significantly. In this case, the momentum-dependent Green's function in Eq. (12) depends on just two macroscopic objects: the band structure  $\epsilon(\mathbf{k})$  and an additional energy function  $\tilde{c}(\mathbf{k}) = \lim_{d \rightarrow 1} \sin(\mathbf{k} \cdot \mathbf{a}) = \tilde{c}$ :

$$g^T(\mathbf{k}; t; t^0) = \exp\left[-\frac{i}{\tilde{c}} \int_{t^0}^t dt \epsilon(\mathbf{k}) \cos \frac{eaA(t)}{\tilde{c}}\right] \\ + \epsilon(\mathbf{k}) \sin \frac{eaA(t)}{\tilde{c}} \int_{t^0}^t dt e^{i(t-t^0)\tilde{c}} \\ \frac{i}{\tilde{c}} \int_{t^0}^t dt \left[ (t - t^0) f(\tilde{c}) \right]; \quad (14)$$

Hence the local Green's function can be found by integrating over a joint density of states<sup>20</sup>

$$\rho(\mathbf{k}; t) = \sum_{\mathbf{k}} \left[ \epsilon(\mathbf{k}) \right] \left[ \tilde{c}(\mathbf{k}) \right]; \quad (15)$$

which yields

$$g_{loc}^T(t; t^0) = \int_{t^0}^t dt \int_{t^0}^t dt^0 \rho(\mathbf{k}; t) g^T(\mathbf{k}; t; t^0); \quad (16)$$

Using the techniques of Mueller-Hartmann<sup>21,22,23</sup> again, gives the following expression for the joint density of states:

$$\rho(\mathbf{k}; t) = \frac{1}{t^2 a^d} \exp\left(-\frac{t^2}{t^2} - \frac{t^2}{t^2}\right); \quad (17)$$

Substituting the joint density of states of Eq. (17) into Eq. (16) and integrating over  $\mathbf{k}$  gives the final expression for the local Green's function:

$$g_{loc}^T(t; t^0) = \frac{i}{\tilde{c}} \int_{t^0}^t dt \left[ (t - t^0) f(\tilde{c}) \right. \\ \left. + \exp\left[-\frac{1}{\tilde{c}} \int_{t^0}^t dt \cos \frac{eaA(t)}{\tilde{c}}\right] \right. \\ \left. + \exp\left[\frac{t^2}{4\tilde{c}^2} - \frac{1}{\tilde{c}} \int_{t^0}^t dt \cos \frac{eaA(t)}{\tilde{c}}\right] \right. \\ \left. + \frac{1}{\tilde{c}} \int_{t^0}^t dt \int_{t^0}^t dt^0 \cos \frac{eaA(t) - A(t^0)}{\tilde{c}} \right] g^0 \\ e^{i(t-t^0)\tilde{c}}; \quad (18)$$

Of course, the result in Eq. (18) agrees with that of Eq. (13) when the vector potential lies along the diagonal.

### III. NUMERICAL RESULTS

We begin by studying the current density of the system in the presence of the electric field. The current operator is determined by the commutator of the polarization operator (defined by  $\mathbf{P} = \sum_i \mathbf{R}_i c_i^\dagger c_i$ ) with the Hamiltonian of the system. The expression for the  $x$ -component of the current-density operator has the following form:

$$j_x = \frac{eat}{\tilde{c}} \sum_{\mathbf{k}} \sin \mathbf{k} \cdot \mathbf{a} \frac{eaA(t)}{\tilde{c}} c_{\mathbf{k}}^y \alpha_{\mathbf{k}}; \quad (19)$$

The expectation value of the  $x$ th component of the current can be easily calculated from the time-ordered Green's function in Eq. (12) in the limit  $t^0 \rightarrow t^+$ :

$$\langle j_x \rangle = \frac{eat}{\tilde{c}} \sum_{\mathbf{k}} \sin \mathbf{k} \cdot \mathbf{a} \frac{eaA(t)}{\tilde{c}} g^T(\mathbf{k}; t; t^+); \\ = \frac{eat^2}{4\tilde{c}} \sum_{\mathbf{k}} \sin \frac{eaA(t)}{\tilde{c}} \frac{d f(\tilde{c})}{d \tilde{c}}(\mathbf{k}); \quad (20)$$

where the summation over momentum is performed the same way as before. The total magnitude of the current density is just  $\tilde{c}$  times this result, since each component along the diagonal is the same. In the limit of low temperature, we perform a Sommerfeld expansion, which gives

$$\langle j_x \rangle = \frac{eat^2}{4\tilde{c}} \sum_{\mathbf{k}} \sin \frac{eaA(t)}{\tilde{c}} \quad (21)$$

[with  $A(t)$  the value of the vector potential for each component]. Note that in the case of a constant field,

$A(t) = Ect$  ( $t$  is a linear function of  $t$ ), and the current is sinusoidal, even though the field is time-independent. This is the well-known Bloch oscillation,<sup>24</sup> with a frequency  $\omega_{\text{Bloch}} = e\hbar E / \hbar^2 k_F$ . Since we have no scattering, the system is a perfect conductor, but the periodicity of the lattice restricts the wavevector to lie in the first Brillouin zone which causes the oscillatory current.

One can investigate a current-current correlation function to determine a noise spectrum, but because the current is periodic, the noise profile would be just two delta functions for a constant field, and we won't learn anything interesting from examining the noise.

It is interesting to note, that the current is nonzero for the case  $A(t) = \text{const}$ , which corresponds to the case of zero electric field. This is a consequence of the fact that the vector potential results in a shifting of the Fermi surface. In the case of an interacting system this current will be destroyed by interparticle scattering. In our case, a free-energy analysis will show that the lowest-energy state is the one without any current. There are a number of analogies of the response of this system to the response of a superconductor (such as an ac response to a dc field, the presence of current-carrying states that do not disappear over time, etc.). All of these results are artifacts of the lack of scattering in the system.

To find the resistivity of the system, we consider the case of a uniform static electric field (along the diagonal) of magnitude  $E$  in  $d$  dimensions, which is turned on at  $t = 0$ , so that  $A(t) = Ect$  ( $t \geq 0$ ),  $\mathbf{E}(t) = E\hat{c}$  ( $t \geq 0$ ), and the potential along a path  $b(1;1;1;\dots) = d$  is equal to  $V = Eb$  (the length  $b$  is the distance over which we have a potential drop). The expression for the Ohm's law in the form  $V = jRa^{d-1}$  (current density multiplied by the resistance-area product), gives the following expression for resistance-area product:

$$Ra^{d-1} = \frac{V}{j} = \frac{4\pi E db}{e^2 a^{d-1} t^2} \sin \frac{eaEt}{\hbar} : \quad (22)$$

The resistivity is defined to be  $1/b$  times the resistance-area product, in the linear-response limit of  $E \rightarrow 0$ . Therefore,

$$\rho_{\text{lin}} = \frac{4\pi d}{e^2 a^{d-1} t^2} : \quad (23)$$

This result is proportional to  $d$ , as it should be because the conductivity is proportional to  $1/d$  in finite dimensions. The correct resistivity is zero for a noninteracting system. Here we see that the linear-response resistivity in Eq. (23) goes to zero in the limit of large time  $t \rightarrow \infty$ .

Let us estimate the linear response resistance of the ballistic metal from the expression in Eq. (23), which can be finite because the linear-response resistance has a factor of  $b = vt$  in it. For the ballistic metal the length  $b$  over which the electrons have moved in the time  $t$  should be  $b = v_F t$ , with  $v_F$  a suitable average of the Fermi velocity.

This gives the resistance

$$R_{\text{lin}} = \frac{4\pi v_F d}{e^2 a^{d-1} t^2} : \quad (24)$$

This expression corresponds to the Sharvin resistance<sup>25,26</sup> for a single-band model in finite dimensions. In three dimensions, the Sharvin resistance is  $R = 2e^2/h$  divided by the number of channels, which is a Fermi surface factor multiplied by  $4\pi k_F^2 A$  area. To compare with our formula, we must first note that we map the hopping integral onto the effective mass (for low electron filling) via

$$t = \frac{\hbar^2 v_F^2}{m a^2} \quad (25)$$

and that  $a^{d-1} t^2 = C$  is a constant of order one (proportional to  $(k_F a)^{d-2}$  for low filling). Therefore,

$$R_{\text{lin}} = \frac{4\pi m v_F a^{d-1}}{e^2 C} / \frac{\hbar}{2e^2 (k_F a)^{d-3}} ; \quad (26)$$

which has a Sharvin-like form (but appears to have the wrong dependence on  $k_F a$  for  $d = 3$ ; this most likely is an artifact of the problems with assuming a spherical Fermi surface in large dimensions, which is valid only for vanishing electron densities).

We can also investigate the heat current carried when there is an electrical field present (but no temperature gradient), and we find that its average value vanishes at half filling, as expected, because the thermopower vanishes at half filling, and we have no thermal gradients to directly drive a thermal current (in the general case, the energy part of the current vanishes, and the chemical potential piece will give a contribution of  $j$  to the heat current). So heat transport is trivial unless one introduces a thermal gradient to the temperature, which we do not do here.

Next we examine the spectral function and the density of states in the presence of a field. The time-dependent spectral function can be calculated from the retarded Green's function  $g^R(t; t^0) = (i\hbar)^{-1} \langle [c(t), c^\dagger(t^0)] \rangle$  (with the operators expressed in a Heisenberg picture) using the Wigner coordinates<sup>27</sup> by introducing the average time  $t_{\text{ave}} = (t + t^0)/2$  and the relative time  $t_{\text{rel}} = t - t^0$  variables. In this case, the spectral function as a function of the average time (and Fourier transformed over the relative time) is equal to

$$A(t_{\text{ave}}; k; ! ) = \frac{1}{\pi} \text{Im} \int_0^\infty dt_{\text{rel}} e^{i! t_{\text{rel}}} g^R(k; t_{\text{ave}}; t_{\text{rel}}); \quad (27)$$

and the DOS is equal to

$$A(t_{\text{ave}}; ! ) = \frac{1}{\pi} \text{Im} \int_0^\infty dt_{\text{rel}} e^{i! t_{\text{rel}}} g_{\text{loc}}^R(t_{\text{ave}}; t_{\text{rel}}); \quad (28)$$

In general, the retarded Green's function can be found from the same technique used to calculate the time-ordered Green's function: first one introduces the time

dependence of the Heisenberg operators, then one evaluates the operator averages. Since the anticommutator of two local creation and annihilation operators (or two operators in the momentum basis) is equal to one, we get

$$g^R(k; t; t^0) = \frac{i}{\hbar} \langle (t - t^0) e^{i(t - t^0)H} \exp \left[ -i \int_{t^0}^t \frac{(k)}{\hbar} dt \cos \frac{eaA(t)}{\hbar C} \right] \exp \left[ -i \int_{t^0}^t \frac{(k)}{\hbar} dt \sin \frac{eaA(t)}{\hbar C} \right] \rangle \quad (29)$$

for the momentum-dependent Green's function and

$$g_{loc}^R(t; t^0) = \frac{i}{\hbar} \langle (t - t^0) e^{i(t - t^0)H} \exp \left[ -i \int_{t^0}^t dt \cos \frac{eaA(t)}{\hbar C} \right] \exp \left[ -i \int_{t^0}^t dt \sin \frac{eaA(t)}{\hbar C} \right] \rangle \quad (30)$$

for the local Green's function (using the  $t$  and  $t^0$  coordinates). Note that these Green's functions have no temperature dependence, hence the spectral function and the DOS are independent of temperature. This is characteristic of a noninteracting system.

The spectral function, in the absence of a field, is a delta function  $A(k; \omega) = \delta(\omega - \epsilon(k))$ . When a field is turned on, the time dependence is no longer a pure exponential, so the spectral function deviates from the delta function, becoming a peaked function of nonvanishing width. In the limit where  $t_{ave} \rightarrow \infty$ , the steady state is approached and the spectral function becomes a set of evenly spaced delta functions, since the Green's function becomes a periodic function in  $t_{rel}$ .

The analysis for the local DOS is more complicated. Since the dependence in Eq. (30) is so simple, the integral can be performed directly, with the result

$$g_{loc}^R(t_{ave}; t_{rel}) = \frac{i}{\hbar} \langle t_{rel} \rangle e^{i t_{rel} = \omega} \exp \left[ -\frac{t^2}{4\hbar^2} \mathcal{J}(t_{ave}; t_{rel})^2 \right]; \quad (31)$$

where

$$I(t_{ave}; t_{rel}) = \int_{t_{ave} - t_{rel} = 2}^{t_{ave} + t_{rel} = 2} dt \exp \left[ -i \frac{eaA(t)}{\hbar C} \right]; \quad (32)$$

In order to evaluate some numerical results, we first consider the case of a constant electric field turned on at

$t = 0$ . In this case, we get

$$I(t_{ave}; t_{rel}) = \langle t_{ave} - t_{rel} = 2 \rangle \langle t_{ave} + t_{rel} = 2 \rangle t_{rel} + \langle t_{ave} - t_{rel} = 2 \rangle \langle t_{ave} - t_{rel} = 2 \rangle \left[ t_{ave} + t_{rel} = 2 + (1 - e^{i \frac{eaE}{\hbar} (t_{ave} - t_{rel} = 2)}) \frac{1}{ieaE} \right] + \langle t_{ave} + t_{rel} = 2 \rangle \langle t_{ave} + t_{rel} = 2 \rangle \left[ (e^{i \frac{eaE}{\hbar} (t_{ave} + t_{rel} = 2)} - 1) \frac{1}{ieaE} t_{ave} + t_{rel} = 2 \right] + \langle t_{ave} + t_{rel} = 2 \rangle \langle t_{ave} - t_{rel} = 2 \rangle \frac{1}{ieaE} (e^{i \frac{eaE}{\hbar} (t_{ave} + t_{rel} = 2)} - e^{i \frac{eaE}{\hbar} (t_{ave} - t_{rel} = 2)}); \quad (33)$$

This result has some interesting properties. If  $E \rightarrow 0$ , then  $I = t_{rel}$  for all  $t_{ave}$ , and  $g_{loc}^R$  is a Gaussian in  $t_{rel}$ , which Fourier transforms to a Gaussian in frequency, i.e., it becomes the noninteracting DOS. There is an interesting scaling behavior. If we define  $t_{ave} = t_{ave} eaE = \tilde{t}$ ,  $t_{rel} = t_{rel} eaE = \tilde{t}$ , and  $\omega = \omega eaE$ , then

$$I(t_{ave}; t_{rel}) = \frac{1}{eaE} I(\tilde{t}_{ave}; \tilde{t}_{rel}); \quad (34)$$

with  $I$  a function independent of  $E$ . Hence

$$g_{loc}^R(t_{ave}; t_{rel}) = \frac{i}{\hbar} \langle t_{rel} \rangle e^{i t_{rel} = \omega} \exp \left[ -\frac{t^2}{4e^2 a^2 E^2} \mathcal{J}(t_{ave}; t_{rel})^2 \right]; \quad (35)$$

and the DOS becomes

$$A(t_{ave}; \omega) = \frac{1}{\pi} \text{Im} \int_0^\infty dt_{rel} e^{i t_{rel} \omega} g_{loc}^R(t_{ave}; t_{rel}); \quad (36)$$

with the normalization chosen so  $\int d\omega A(\omega) = 1$  (for easier comparison of curves for different  $E$ ). Hence we expect the DOS to have the same shape as a function of  $\omega$  (with a possible shift due to the chemical potential factor), but the amplitude of the oscillations grows as  $E$  increases [because of the minus sign in the exponent in Eq. (35)]. But that turns out only to be true near  $\omega = 0$ . At other frequencies, the evolution with  $E$  is not always monotonic, because the DOS conserves total spectral weight, so there cannot be a monotonic evolution of the peaks at all frequencies.

Note that the DOS satisfies two properties in equilibrium. The first is that the integral over frequency equals 1. The second is that the DOS is always positive. The proof for the integral yielding 1 holds even in the nonequilibrium case, because the anticommutator of two Fermionic creation and annihilation operators at the same time is still one. The positivity does not hold, because the standard derivation, using the spectral representation, requires the Hamiltonian to be independent of time in order to be able to be used, and thereby prove the positivity. Indeed, the DOS in the presence of a field has regions where it is negative.

It is interesting to consider the limit of large  $t_{ave}$ , i.e.,  $t_{ave} \rightarrow \infty$ , then we get the steady-state solution. We

take only the last term of  $I(t_{\text{ave}}; t_{\text{rel}})$  in Eq. (33) because  $t_{\text{ave}}$  is always larger than  $t_{\text{rel}}$  in this limit. The Green's function becomes

$$g_{\text{loc}}^R(t_{\text{ave}} \rightarrow 1; t_{\text{rel}}) = \frac{i}{\omega} \exp\left(\frac{t^2}{2e^2 a^2 E^2}\right) \cos\left(\frac{eaE}{\omega} t_{\text{rel}}\right) \quad (37)$$

The Fourier transform of this is a set of delta functions, with different amplitudes, that are equally spaced in frequency, with a spacing  $eaE/\omega$  (since the Green's function is periodic in  $t_{\text{rel}}$ ). This is the famous Wannier-Stark ladder<sup>17</sup>, expected for system placed in an external electric field. In the results plotted in Fig. 1, the fact that the peaks at multiples of this frequency get larger, and grow in height as  $t_{\text{ave}}$  grows, indicates our results are showing the correct build-up to the steady state, but they will never get there until  $t_{\text{ave}} \rightarrow 1$ . It is no coincidence that this frequency is the same as the Bloch oscillation frequency. This discussion was first described in detail from the Green's function approach by Davies and Wilkins<sup>16</sup>. Note that the DOS is nonnegative in the steady state.

We can calculate the weight of the delta functions by performing the Fourier series integral. The frequencies are  $N eaE/\omega$ , and the Fourier coefficient is

$$\begin{aligned} w_N &= \frac{2}{eaE} \int_0^{2\pi} dt_{\text{rel}} \cos\left(\frac{N eaE}{\omega} t_{\text{rel}}\right) \exp\left(\frac{t^2}{2e^2 a^2 E^2}\right) \cos\left(\frac{eaE}{\omega} t_{\text{rel}}\right) \\ &= \frac{2\pi}{e^2 a^2 E^2} \int_0^{2\pi} du \cos(Nu) \exp\left(\frac{t^2}{2e^2 a^2 E^2}\right) \cos u \quad (38) \end{aligned}$$

For our numerical results, we examine how the system approaches the steady state as the field is turned on. We work at half filling ( $\nu = 0$ ), where the DOS is symmetric; hence, we plot only the results for positive frequencies. The field needs to be large enough for our calculations to be able to see the nonlinear effects of the field on the DOS. For us, the numerical results can easily see effects on the DOS when  $eaE/\omega > 0.1$ . In Fig. 1, we plot results for  $eaE/\omega = 1$ . While it is true that the Green's functions for  $t$  and  $t^0$  both less than zero are equal to their equilibrium (field-free) limit, the Wigner DOS feels the effect of the fields for all finite  $t_{\text{ave}}$ , because the integral over  $t_{\text{rel}}$  always includes some Green's functions with either  $t$  or  $t^0$  larger than zero. We can see that significant "precursor" effects occur only for  $t_{\text{ave}} > 2$  here, and the DOS develops significant oscillations before one can see the delta functions start to build up at the integer frequencies.

We plot a close up of the region around  $\omega = 1$  in Fig. 2. Note how a sharp peak develops as the average time increases, but there are significant oscillations near  $\omega = 1$  whose amplitude decreases slowly as  $t_{\text{ave}}$  increases.

In Fig. 3, we plot the DOS in the  $\omega$  variable near  $\omega = 0$  for  $t_{\text{ave}} = 100$  and for various values of  $eaE/\omega$  (0.1, 0.3, 1.0,

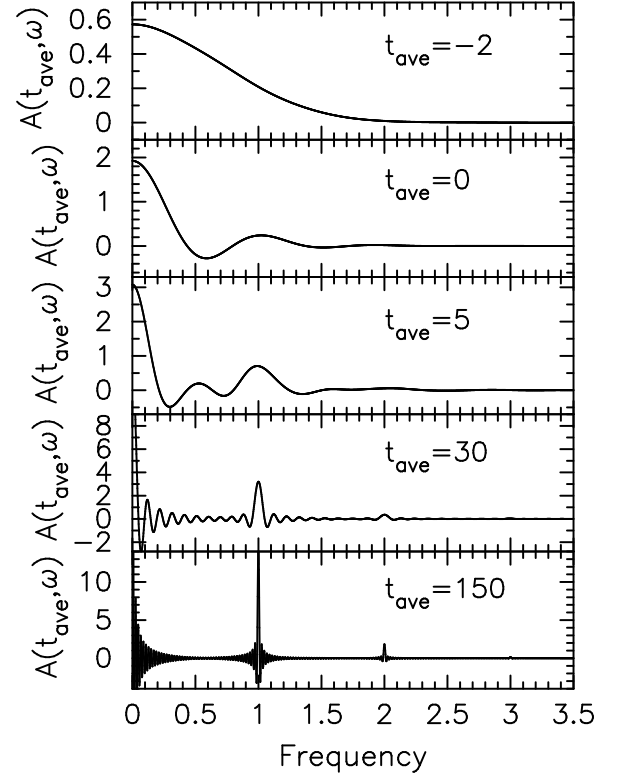


FIG. 1: Density of states  $A(t_{\text{ave}}; \omega)$  for the noninteracting electrons with  $eaE/\omega = 1$ . Note how the DOS is essentially a Gaussian for  $t_{\text{ave}} < 2$ , but then develops large oscillations as  $t_{\text{ave}}$  increases. The DOS approaches a steady state for large time given by a set of delta functions, equally spaced by the Bloch oscillation frequency. The DOS is no longer positive once the field is turned on, but the integral does always equal 1.

3.0, and 10.0). This shows how the oscillations grow as  $E$  increases. For other integer values of  $\nu$ , the evolution is not monotonic in the field strength  $E$  (for example, at  $\nu = 1$  the peak values increase with  $E$  for  $0.1 < eaE/\omega < 0.7$  and then decrease for  $0.7 < eaE/\omega < 10$ ).

In addition to the spectral function and the DOS, it is interesting to examine the distribution function. In equilibrium, the distribution function is a Fermi-Dirac distribution function, but the distribution function can change for nonequilibrium cases. In order to discuss distribution functions, we need to define two more Green's functions—the so-called lesser and greater Green's functions. They are defined as  $g^<(t; t^0) = (i/\hbar) \langle c(t) c^\dagger(t^0) \rangle$  and  $g^>(t; t^0) = (i/\hbar) \langle c^\dagger(t^0) c(t) \rangle$  (with the operators expressed in a Heisenberg picture). These Green's functions can also be determined exactly for Bloch electrons, and their expressions are the same as those for the retarded Green's function in Eqs. (29) and (30), except the  $(t - t^0)$  factor is replaced by  $f(k)$  for  $g^<$  and by  $[1 - f(k)]$  for  $g^>$ . There are three cases for the distribution function that we can consider (the Wigner distribution, the quasiparticle distribution, and the local

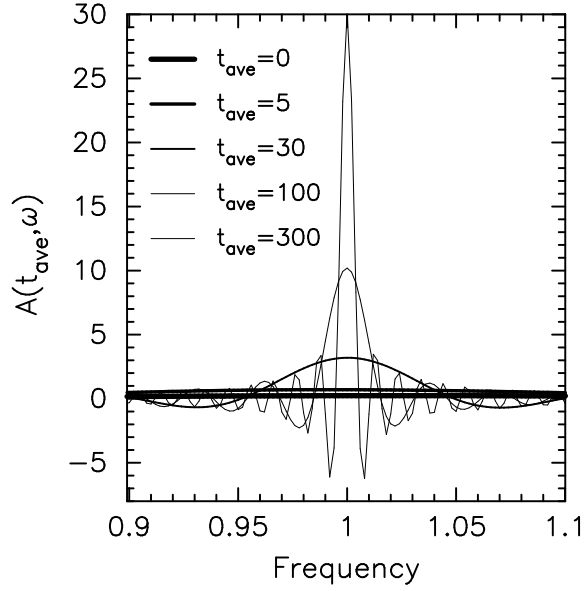


FIG. 2: Close up of the density of states  $A(t_{\text{ave}}; !)$  near  $! = 1$  for the noninteracting electrons with  $eaE \approx 1$ . Note how the DOS approaches a steady state for large time by developing a sharp peak, but that there are significant oscillations near the sharp peak that decay slowly in time.

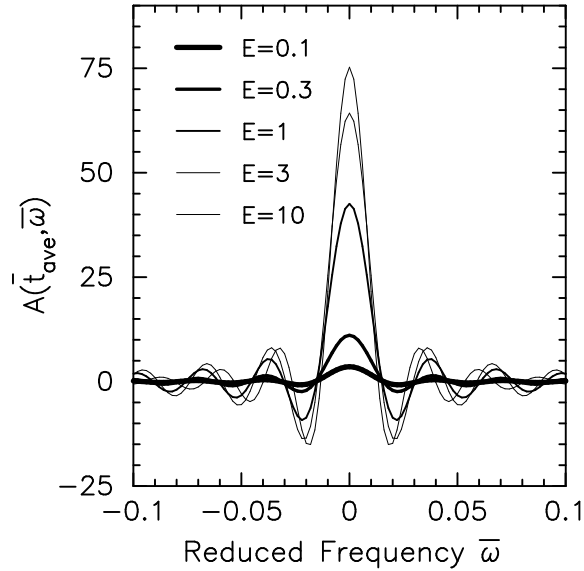


FIG. 3: Close up of the density of states  $A(t_{\text{ave}}; !)$  near  $! = 0$  for the noninteracting electrons with  $eaE \approx 0.1, 0.3, 1.0, 3.0$ , and  $10.0$ . Note how the peak in the DOS evolves as a function of the electric field.

quasiparticle distribution). The most often used distribution function is the Wigner distribution function, defined to be

$$f_{\text{Wigner}}(t_{\text{ave}}; \mathbf{k}) = i^{-1} g^<(\mathbf{k}; t = t_{\text{ave}}; t^0 = t_{\text{ave}}): \quad (39)$$

The Wigner distribution function is always equal to the

field-free FermiDirac result  $f_{\text{Wigner}}(t_{\text{ave}}; \mathbf{k}) = f(\mathbf{k})$  for Bloch electrons. The quasiparticle distribution function is defined in analogy with the equilibrium result  $[g^<(\mathbf{k}; !)] = 2 \text{ if } (!) A(\mathbf{k}; !)]$  via

$$f_{\text{quasi}}(t_{\text{ave}}; \mathbf{k}) = \frac{1}{2} \frac{\text{Im } g^<(t_{\text{ave}}; \mathbf{k}; !)}{A(t_{\text{ave}}; \mathbf{k}; !)} \quad (40)$$

(note that the name quasiparticle distribution does not necessarily imply that there must be an underlying Fermi liquid in the system). Since the only difference between the retarded Green's function and the lesser Green's function is the replacement of the theta function by the FermiDirac distribution (which does not depend on the time variables), the ratio of the two terms in Eq. (40) has an explicit factor of  $f(\mathbf{k})$ . The Fourier transform of the numerator is over all  $t_{\text{rel}}$ , while the denominator is only over all positive  $t_{\text{rel}}$ . The integral  $I(t_{\text{ave}}; t_{\text{rel}})$  is an odd function of  $t_{\text{rel}}$  [see Eq. (32)], which implies the numerator in Eq. (40) is  $2 f(\mathbf{k}) A(t_{\text{ave}}; \mathbf{k}; !)$ , and we find the quasiparticle distribution function is equal to the FermiDirac distribution once again. The final distribution function to be defined is the local quasiparticle distribution function. This is

$$f_{\text{quasi}}^{\text{loc}}(t_{\text{ave}}) = \frac{1}{2} \frac{\text{Im } g_{\text{loc}}^<(t_{\text{ave}}; !)}{A(t_{\text{ave}}; !)}: \quad (41)$$

This distribution function is nontrivial in a field, because the DOS and the lesser Green's function both have oscillations, but the zeros occur at different locations on the frequency axis, so the ratio in Eq. (41) can have significant oscillations.

The calculation of the local quasiparticle distribution function is difficult because the presence of an  $f(\mathbf{k})$  factor precludes us from performing the integral over analytically; hence the numerical computations are more involved. We need to evaluate the integral

$$g^<(t_{\text{ave}}; t_{\text{rel}}) = \frac{i}{\pi} \int_{-\infty}^{\infty} d\omega f(\omega) \exp\left[-i\omega(t_{\text{ave}}; t_{\text{rel}}) - \frac{t^2}{4\tau^2} Y^2(t_{\text{ave}}; t_{\text{rel}})\right] \quad (42)$$

numerically. If  $eaE \approx 0$ , then this is just the Fourier transform of  $2 \text{ if } (!) (!)$ , which gives the correct lesser function. If  $eaE \approx \neq 0$ , then the Green's function has to be calculated numerically. Because the real part of the lesser Green's function is nonzero for a longer range in time than the imaginary part, the function  $g^<$  will have more oscillations than the  $g^R$  function. The results for a local quasiparticle distribution function are plotted in Fig. 4. As it follows from this figure, the local quasiparticle distribution function varies significantly from the equilibrium values as  $t_{\text{ave}}$  increases. This is because the  $g^<$  Green's function has high frequency oscillations, which are not as strong in the DOS. The oscillations continue as  $t_{\text{ave}}$  increases, but they become difficult to plot.

Of course the momentum-dependent quasiparticle distribution function is equal to the Fermi-Dirac distribution function for this problem.

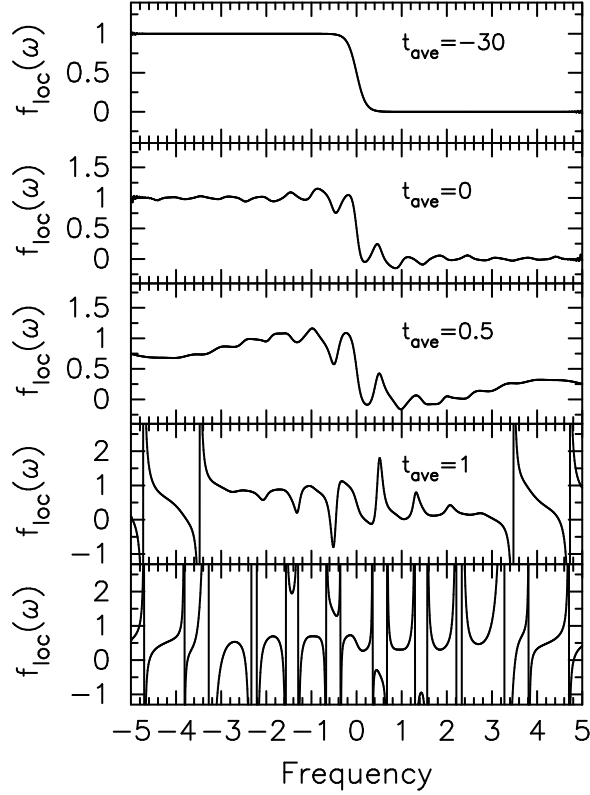


FIG. 4: Local quasiparticle distribution function  $f_{\text{loc}}(\omega; t)$  for noninteracting electrons with  $eaE = 1$  and  $T = 0.1$ . Note how the local quasiparticle distribution function varies significantly from the equilibrium values as  $t_{\text{ave}}$  increases (the lowest panel is for  $t_{\text{ave}} = 2$ ). This is because the  $g^c$  Green's function has high frequency oscillations, which are not as strong in the DOS. The oscillations continue as  $t_{\text{ave}}$  increases, but they become difficult to plot.

Finally, we study the time dependence of the DOS for the case of a sharp pulse during the period of time  $0 < t < t_E$ . The second derivative of the vector potential is proportional to the strength of the magnetic field (which we are neglecting), so we want to keep the second derivative small for the calculations to make sense. We choose the electric field to have the following time dependence:  $E(t) = E(t_E - t)(t)$ , which corresponds to a vector potential

$$A(t) = -eEt(t_E - t)(t) - eEt_E(t - t_E): \quad (43)$$

Note that these results are "singular" for the noninteracting case, because the total vector potential is a constant that can correspond to a current-carrying state if the Fermi surface is shifted from the zone center. Because there is no scattering, such a current lives forever (but would decay in the presence of any scattering). Numerical calculations show that the DOS deviates visibly from

its equilibrium value during the times  $t < t_{\text{relax}}$  when the amplitude of the field is larger or on the order of  $t$ ; the relaxation time  $t_{\text{relax}}$  is on the order of the pulse time  $t_E$ .

The results of the calculations are presented in Fig. 5 for  $eaE = 1$  (when  $eaE$  is much smaller than 1, the oscillations become hard to see). The nonequilibrium DOS shows oscillating behavior, which then decays as time increases. The results satisfy a symmetry relation, where the Wigner DOS is identical for  $t_{\text{ave}}$  and  $t_{\text{ave}}^0$  when  $t_{\text{ave}} + t_{\text{ave}}^0 = t_E$ .

We also consider the case of a smooth pulse with a smooth turn-on and turn-off of the electric field:  $A(t) = Et_E \exp(-t^2/t_E^2)/2$  [which corresponds to an electric field  $E(t) = Et/t_E \exp(-t^2/t_E^2)$ ]. This field changes sign at  $t = 0$  and has its maximum amplitude at  $t = \pm 0.5$ . The Wigner DOS is symmetric in  $t_{\text{ave}}$ , so we only plot results for positive times in Fig. 6. Note that at  $t_{\text{ave}} = 0$  the field has been on for a long time, so the result is far from a Gaussian. The amplitude of the peak in the DOS at  $\omega = 0$  is largest at  $t_{\text{ave}} = 0.5$ , and decays rapidly for larger times.

The proof of the symmetry relation for the Wigner DOS is rather straightforward to do. If the vector potential  $A(t)$  has definite parity:  $A(-t) = \pm A(t)$ , then it is easy to see from Eq. (32) that  $I(t_{\text{ave}}; t_{\text{rel}}) = I(t_{\text{ave}}; t_{\text{rel}})$  for even functions and  $I(t_{\text{ave}}; t_{\text{rel}}) = -I(t_{\text{ave}}; t_{\text{rel}})$  for odd functions. Since it is the modulus of  $I$  that enters into the calculation of  $A(t_{\text{ave}}; !)$ , the DOS will satisfy the given symmetry rules. For the case of the constant-field pulse, we need to shift the time axis by  $t_E/2$  and shift the vector potential by  $E t_E/2$  to have a vector potential that is odd in time. The shift of the vector potential has no effect on the modulus of  $I$ , since it contributes only a phase, while the shift in the time axis is precisely what is needed to give the symmetry relation described above. For the Gaussian pulse, the vector potential is already an even function, and the symmetry relation follows directly.

Note that we do not calculate the experimental probe of the reactivity as a function of time after the initial pulse, because this system has no intrinsic scattering, so the optical conductivity is always a delta function peak at zero frequency, hence we would not learn anything interesting from such an exercise here. It would be interesting to probe such behavior in systems with intrinsic scattering mechanisms, to understand how the different relaxation mechanisms can be detected.

#### IV. CONCLUSIONS

We have studied the nonlinear response of Bloch electrons to an external time-varying (but spatially homogeneous) electric field by employing an exact nonequilibrium formalism on an infinite-dimensional hypercubic lattice. We found that the current showed Bloch oscillations, even when the electric field was constant in time, and we derived a form for the Sharvin-like resistance of



the system.

The time-dependence of the DOS was calculated. We showed that it becomes a Wannier-Stark ladder for long times, but the transient evolution toward those discrete delta functions had a complex structure, that survives out to long times. We also examined a number of different kinds of distribution functions, and showed that the most commonly chosen distribution functions retained the Fermi-Dirac form regardless of the strength of the electric field (but the local quasiparticle distribution shows complex oscillatory behavior). For pulsed fields, we saw the transient response build and then decay. The amplitude of the oscillations was proportional to the amplitude of the electric field  $E$  for a wide range of field strengths, and we needed the field to be sufficiently large ( $eaE \sim \tau$ ) before they could be easily seen. Of course,

the oscillations decay at times larger than the pulse time.

These noninteracting Green's functions form the basis for a nonequilibrium dynamical mean field theory, which we are currently developing to study the nonlinear response of systems close to the Mott transition. Results of that work will appear elsewhere.

#### Acknowledgments

We would like to thank J. Serene and V. Zlatić for useful discussions. We acknowledge support from the National Science Foundation under grant number DMR-0210717 and the Office of Naval Research under grant number N00014-99-1-0328.

- 
- Electronic address: [turk@physics.georgetown.edu](mailto:turk@physics.georgetown.edu);  
URL: <http://www.physics.georgetown.edu/~turk>
- <sup>y</sup> Electronic address: [freericks@physics.georgetown.edu](mailto:freericks@physics.georgetown.edu);  
URL: <http://www.physics.georgetown.edu/~jkf>
- <sup>1</sup> R. Kubo, J. Phys. Soc. Japan 12, 570 (1957).
  - <sup>2</sup> D. A. Greenwood, Proc. Phys. Soc. (London) 71, 585 (1958).
  - <sup>3</sup> S. K. Sarker, J. H. Davies, F. S. Khan, and J. W. Wilkins, Phys. Rev. B 33, 7263 (1986).
  - <sup>4</sup> F. S. Khan, J. H. Davies, and J. W. Wilkins, Phys. Rev. B 36, 2578 (1987).
  - <sup>5</sup> P. Lipavsky, F. S. Khan, F. Abdolsalam, and J. W. Wilkins, Phys. Rev. B 43, 4885 (1991).
  - <sup>6</sup> P. Lipavsky, F. S. Khan, A. Kalvova, and J. W. Wilkins, Phys. Rev. B 43, 6650 (1991).
  - <sup>7</sup> P. Lipavsky, F. S. Khan, and J. W. Wilkins, Phys. Rev. B 43, 6665 (1991).
  - <sup>8</sup> L. P. Kadanoff and G. Baym, Quantum Statistical Mechanics (Benjamin, New York, 1962).
  - <sup>9</sup> L. V. Keldysh, Zh. Eksp. Teor. Fiz. 47, 1945 (1964).
  - <sup>10</sup> L. V. Keldysh, Sov. Phys. JETP 20, 1018 (1965).
  - <sup>11</sup> G. Baym, Progress in Nonequilibrium Green's Functions (World Scientific, New Jersey, 2000), p. 17.
  - <sup>12</sup> L. V. Keldysh, Progress in Nonequilibrium Green's Functions II (World Scientific, New Jersey, 2003), p. 4.
  - <sup>13</sup> J. Rammer and H. Smith, Rev. Mod. Phys. 58, 323 (1986).
  - <sup>14</sup> A. P. Jauho and J. W. Wilkins, Phys. Rev. Lett. 49, 762 (1982).
  - <sup>15</sup> A. P. Jauho and J. W. Wilkins, Phys. Rev. B 29, 1919 (1984).
  - <sup>16</sup> J. H. Davies and J. W. Wilkins, Phys. Rev. B 38, 1667 (1988).
  - <sup>17</sup> G. H. Wannier, Rev. Mod. Phys. 34, 645 (1962).
  - <sup>18</sup> W. Metzner and D. Vollhardt, Phys. Rev. Lett. 62, 324 (1989).
  - <sup>19</sup> P. Schmidt and H. Monien (2002), cond-mat/0202046.
  - <sup>20</sup> P. Schmidt (2002), Diplom Thesis, University of Bonn (unpublished).
  - <sup>21</sup> E. Müller-Hartmann, Z. Phys. B 74, 507 (1989).
  - <sup>22</sup> E. Müller-Hartmann, Z. Phys. B 76, 211 (1989).
  - <sup>23</sup> E. Müller-Hartmann, Int. J. Mod. Phys. B 3, 2169 (1989).
  - <sup>24</sup> N. W. Ashcroft and N. D. Mermin, Solid State Physics (Holt, Rinehart and Winston, Philadelphia, 1976).
  - <sup>25</sup> Y. V. Sharvin, Zh. Eksp. Teor. Phys. 48, 984 (1965).
  - <sup>26</sup> Y. V. Sharvin, Sov. Phys. JETP 21, 655 (1965).
  - <sup>27</sup> E. P. Wigner, Phys. Rev. 40, 749 (1932).

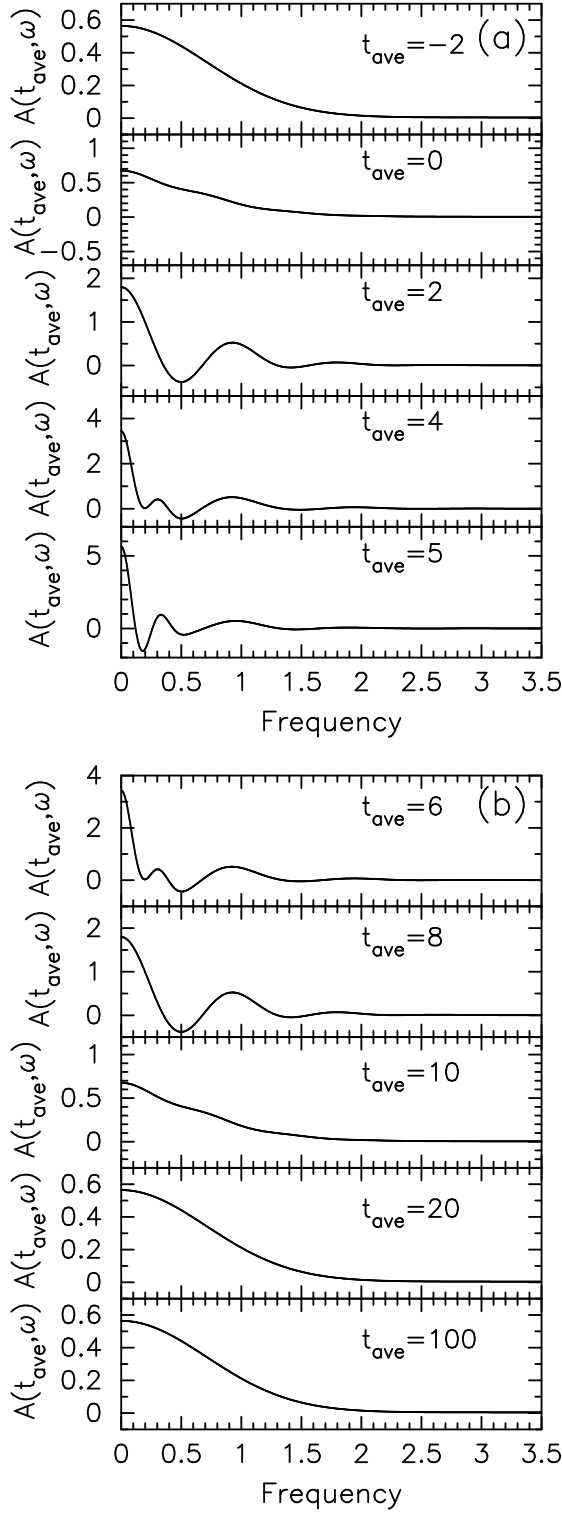


FIG. 5: Local DOS for the case of a sharp  $\delta$  pulse with  $eaE = 1.0$ ,  $t_E = 10.0$ , and various average times. The horizontal scale is the same in every panel, but the vertical scale changes in the different panels. By comparing figure (a) with figure (b), one can see that the response is identical for times  $t_{\text{ave}}$  and  $t_{\text{ave}}^0$  that satisfy  $t_{\text{ave}} + t_{\text{ave}}^0 = t_E$ .

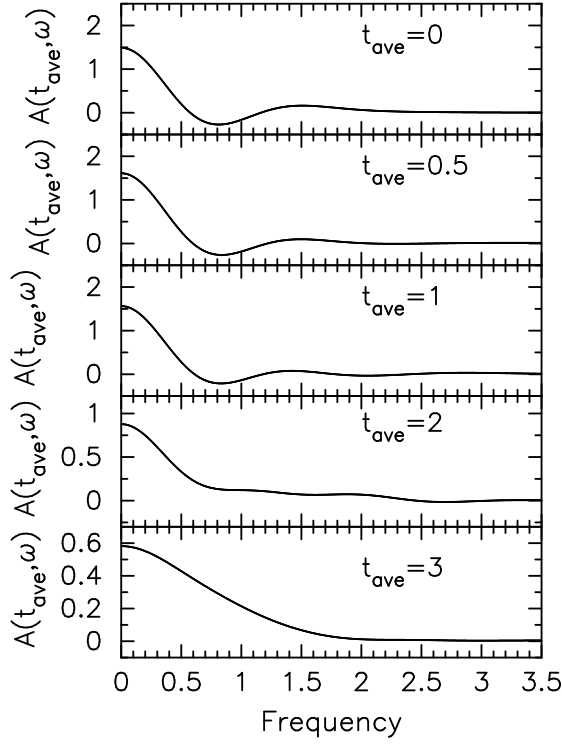


FIG. 6: Local DOS for the case of a smooth Gaussian pulse with  $eaE = 10.0$ ,  $t_E = 1.0$ , and various average times. The results are completely symmetric between negative and positive average times, so we plot only the positive times here. Note how the oscillations are already strong at  $t_{ave} = 0$ , first increase slightly, then fade away as the average time increases.